

---

# CrowdMoGen: Zero-Shot Text-Driven Collective Motion Generation

---

Xinying Guo Mingyuan Zhang Haozhe Xie Chenyang Gu Ziwei Liu✉

S-Lab, Nanyang Technological University

✉ corresponding author

<https://gxyes.github.io/projects/CrowdMoGen.html>



Figure 1: **CrowdMoGen** is a zero-shot, text-driven framework that enables generalizable planning and generation of crowd motions. Given a scene context, we aim to generate realistic crowd motions that fit the scene settings. The motions above are generated by the proposed **CrowdMoGen**.

## Abstract

*Crowd Motion Generation* is essential in entertainment industries such as animation and games as well as in strategic fields like urban simulation and planning. This new task requires an intricate integration of control and generation to realistically synthesize crowd dynamics under specific spatial and semantic constraints, whose challenges are yet to be fully explored. On the one hand, existing human motion generation models typically focus on individual behaviors, neglecting the complexities of collective behaviors. On the other hand, recent methods for multi-person motion generation depend heavily on pre-defined scenarios and are limited to a fixed, small number of inter-person interactions, thus hampering their practicality. To overcome these challenges, we introduce **CrowdMoGen**, a zero-shot text-driven framework that harnesses the power of Large Language Model (LLM) to incorporate the collective intelligence into the motion generation framework as guidance, thereby enabling generalizable planning and generation of crowd motions without paired training data. Our framework consists of two key components: **1) Crowd Scene Planner** that learns to coordinate motions and dynamics according to specific scene contexts or introduced perturbations, and **2) Collective Motion Generator** that efficiently synthesizes the required collective motions based on the holistic plans. Extensive quantitative and qualitative experiments have validated the effectiveness of our framework, which not only fills a critical gap by providing scalable and generalizable solutions for *Crowd Motion Generation* task but also achieves high levels of realism and flexibility.

# 1 Introduction

*Crowd Motion Generation* holds significant potential across various fields, notably in entertainment, and urban simulation and planning. Despite its importance, current techniques predominantly address crowd dynamics through simulations rather than actual motion generation. These traditional methods often reduce individuals within crowds to simplistic particle models that only account for trajectories without detailed, context-specific motions. Alternatively, they rely on basic, non-transferable rule-based motion patterns that are tightly bound to specific scenarios. Such approaches, therefore, do not genuinely generate crowd motions; they merely simulate them on a rudimentary level. This limitation reveals a clear gap in research focused on the generation of diverse and adaptable crowd motions that can be tailored to meet user-specific requirements. Addressing this gap, our work takes a pioneering step forward by defining the task of *Crowd Motion Generation* as the creation of crowd motions in response to textual descriptions that specify user needs, and we introduce **CrowdMoGen**, a zero-shot text-driven framework designed to generate authentic and flexible crowd motions.

Current single motion generation methods now incorporate multi-modal controls, including action categories [15, 41], text [14, 68], music [52, 12], and hybrid inputs [70]. However, these approaches encounter scaling issues in multi-person scenarios due primarily to inadequate handling of complex inter-human interactions. Furthermore, existing multi-person motion generation techniques generally rely on datasets that feature only two interacting individuals [9, 6, 28] or are constrained to limited pre-defined scenarios [73]. Consequently, these methods not only confront challenges in scaling to larger crowds but also demonstrate limited adaptability to more general scenes that require varied interactions and dynamic crowd behaviors.

There are two primary challenges in addressing the *Crowd Motion Generation* task. **1)** There is a marked scarcity of crowd datasets with paired data. Current multi-person datasets are often limited in size [32], feature only a fixed and small number of participants [9, 6, 28], have restricted themes [73], and lack comprehensive annotations [38]. **2)** As crowd sizes increase, effectively modeling the complex interactions among numerous individuals and generating their movements becomes challenging but crucial.

To address these challenges, we propose **CrowdMoGen**, a novel two-stage, zero-shot framework for *Crowd Motion Generation*, which separates motion decision-making from motion generation into two distinct tasks. **1) Crowd Scene Planner** uses a Large Language Model (LLM) to interpret and decide on crowd movements based on user scenarios, giving our method zero-shot capabilities. It provides detailed semantic attributes (like action categories) and spatial attributes (like trajectories and interactions) for each individual, managing both overall crowd dynamics and individual interactions. **2) Collective Motion Generator** enhances the realism of generated motions and ensures strict adherence to control signals through joint-wise *InputMixing*, customized *ControlAttention* mechanisms, and carefully designed training objectives.

The primary contributions are as follows:

- 1)** We introduce the concept of *Crowd Motion Generation*, which integrates strategic motion planning with advanced control mechanisms to create realistic crowd scenes tailored to user requirements.
- 2)** We propose **CrowdMoGen**, which leverages LLM to provide zero-shot capabilities, effectively addressing the *Crowd Motion Generation* task by separating motion decision-making from motion generation into two distinct sub-goals.
- 3)** Extensive quantitative and qualitative evaluations demonstrate the effectiveness of our method. It fills the research gap by achieving high realism and flexibility in generating crowd motions.

## 2 Related Works

**Human Motion Generation.** Variational Autoencoders (VAEs) and diffusion models are widely used in motion generation, leveraging diverse control prompts to create high-quality human motions. Motion prediction [13, 53, 16, 4, 2, 1, 11, 62, 58, 37, 5, 7, 22, 54], for example, generate complete sequences from incomplete historical data or partial movements, ensuring the generated motions are smooth and realistic. A range of external controls, such as action categories [15, 41, 72, 25], music [27, 74, 52, 39, 63], text [42, 56, 57, 24, 3, 34, 71, 50, 35, 47, 68, 21, 19, 64, 43, 30, 69], scenes [20, 29, 33, 60], objects [10, 26, 55, 17, 31, 44, 40, 51], and trajectories [23, 46], further

allows for stylized and customized motions. Additionally, recent innovations have introduced unified motion models [70] that combine multi-modal inputs and multitask learning to enhance the versatility and controllability of individual human motion generation.

Recently, multi-person motion generation has gained increased attention. Some methods, like unsupervised motion completion for groups [73], fail to capture the semantic and spatial dynamics of interactions due to reliance on limited-themed datasets lacking comprehensive annotations. Moreover, while two-person text-motion datasets such as DLP [6] and InterHuman [28] have been introduced, methods depending on them effectively model pairwise interactions but struggle to extend to larger groups, failing to address broader inter-human dynamics. InterControl [59] makes initial strides to create multi-person interactions by explicitly controlling joint positions as per predefined motion plans, but its effectiveness diminishes in scenarios involving more than two people or larger crowds due to requiring heavy manual work.

Consequently, existing methods expose significant shortcomings in realistically generating crowd motions, highlighting the need for more adaptable and logical motion planning, as well as efficient motion controlling and generation strategies.

**Controllable Motion Generation with Diffusion Models.** *Crowd Motion Generation* requires precise management of crowd dynamics and individual motion semantics, with the integration of spatial constraints into text-driven motion generation model posing significant challenges. Successful methods need to align with textual descriptions, adhere to spatial controls, maintain natural motion, and respect human body prior. Existing methods like MDM [57] and PriorMDM [48], which rely on inpainting techniques, predict missing motion components from observed data but often fail to effectively manipulate joints other than the pelvis or handle sparse spatial constraints. GMD [23] addresses the issue of sparse guidance with dense guidance propagation technique yet struggles to flexibly control spatial constraints across various joints and frames. OmniControl [61] and InterControl [59] utilize a hybrid method combining classifier guidance with a ControlNet [67], enhancing spatial signal integration and control accuracy. However, this approach impacts the realism of the motion. Inspired by these insights, we designed a transformer-based diffusion model that incorporates efficient control signal processing, a customized attention mechanism, and robust joint loss propagation. This configuration achieves an optimal balance between high-quality motion generation and precise model control capabilities.

### 3 Methodology

As illustrated in Figure 2, our innovative framework, **CrowdMoGen**, enables the flexible creation of crowd scenes customized to diverse requirements. The structure of the following subsections is as follows: Section 3.1 outlines the architecture and key functionalities of **CrowdMoGen**. In Section 3.2, we detail the design and function of our **Crowd Scene Planner**, which converts diverse crowd scene requirements into unified control signals. Finally, Section 3.3 explores how these control signals are utilized to generate controllable human motions using our **Collective Motion Generator**, thereby synthesizing realistic crowd scenes.

#### 3.1 Framework Overview

**Problem Definition.** We define the task of *Crowd Motion Generation* as the creation of crowd motions in response to textual scene descriptions. Formally, given a textual scene description  $\mathcal{T}_{scene}$  and a specified total number of people  $N$ , the objective is to generate a crowd motion  $\Theta$  not only aligns with the textual scene description  $\mathcal{T}_{scene}$  but also appears natural and coherent. In this context,  $\Theta \in \mathbb{R}^{N \times F \times D}$  defines the generated crowd motion, where  $F$  is the number of motion frames and  $D$  is the dimension of individual motion representation per frame.

**Overall Framework.** Due to the complexity of crowd motion in both semantic and spatial aspects, this task requires strategic motion planning and advanced control mechanisms to ensure qualified generation results. In the initial stage of our framework, the extensive prior knowledge of crowd motions from GPT-4 enables the development of our **Crowd Scene Planner**  $\mathcal{P}$ . This planner addresses the inherent uncertainties in crowd scenarios by generating detailed, stochastic execution plans  $\mathcal{C}_{plan} = (\mathcal{C}^s, \mathcal{C}^t)$  for the crowd based on scene descriptions  $\mathcal{T}_{scene}$ . Specifically,  $\mathcal{C}^s \in \mathbb{R}^{N \times F \times 3}$  outlines the spatial joint and path plans for individuals, formatted in a global keypoint motion

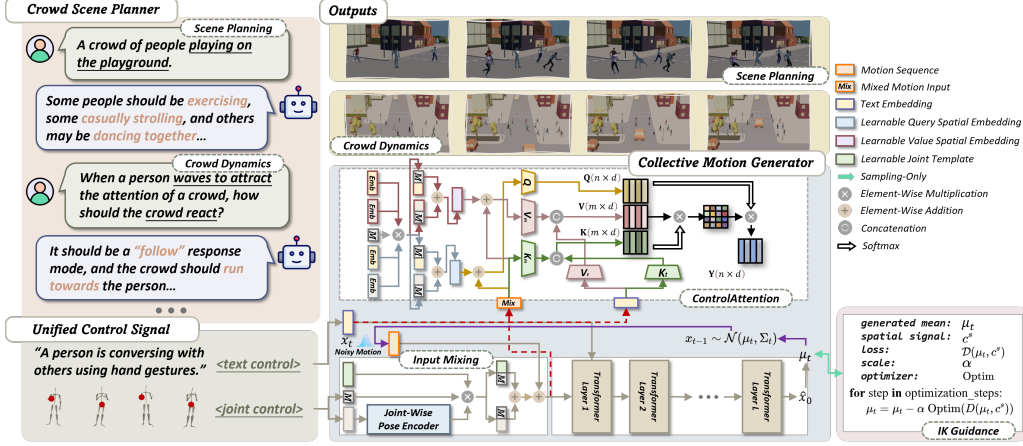


Figure 2: **Overview of CrowdMoGen.** The **CrowdMoGen** framework comprises two main components: **1) Crowd Scene Planner**, which uses a Large Language Model (LLM) to interpret and arrange crowd motions based on textual requirements from the user. This component then provides unified control signals in both textual and spatial formats. **2) Collective Motion Generator**, which leverages these control signals to manipulate and generate realistic individual motions.

representation. Concurrently,  $C_n^t, n \in [1, N]$  provides semantic motion descriptions to guide each individual. Using a tree-of-thought approach enhances the planner’s ability to systematically organize crowd dynamics. For instance, given the description  $\mathcal{T}_{scene}$  as "a group of people on a playground" with a specific number of people  $N$ ,  $\mathcal{P}$  organizes the crowd into interaction groups, assigns relevant activities like dancing, exercising, or walking, and imposes spatial constraints for group positioning, movement trajectory, and joint interactions. The output plan integrates textual motion descriptions  $C^t$  with spatial guidelines  $C^s$ , forming comprehensive control signals for each individual’s movement. In the second stage, a **Collective Motion Generator**  $\mathcal{G}$  takes over and accurately generates individual motions based on the crowd motion control plan  $C_{plan} = (C^s, C^t)$ , thereby generating the crowd motion that precisely conform to scene requirement  $\mathcal{T}_{scene}$  in a zero-shot manner.

### 3.2 Crowd Scene Planner

In this section, we detail the **Crowd Scene Planner** module, which is capable of both macroscopic and microscopic control over crowd motions, as illustrated in Figure 2.

**Scene Parameters.** In both control modes, we establish specific scene hyper-parameters,  $C_{params}$ , to determine the initial rough layout of the scene. These parameters include the total number of individuals  $N$ , crowd density  $P$ , average group size  $G$ , and the intensity of crowd interactions  $I$ . Average group size indicates whether individuals tend to form larger or smaller interaction groups, while the intensity of crowd interactions measures the level of physical contact, ranging from strong to weak. Users have the option to manually set these parameters or allow the planner to automatically adjust them according to the provided scene descriptions.

**Macroscopic Control.** Effective macroscopic control is crucial for accurately simulating vivid and dynamic crowd motions. We initiate the process by inputting a textual scene description  $\mathcal{T}_{scene}$  containing the current state of the crowd,  $C_t$ , and any perturbations,  $P_t$ . Based on this  $\mathcal{T}_{scene}$ , the planner  $\mathcal{P}$  generates a plan  $C_{plan} = (C^s, C^t)$  to guide the evolution of subsequent crowd states. We have identified six principal crowd response patterns to various disturbances: **1) Following**, where the crowd follows a leader; **2) Avoiding**, involving the crowd dodging a fast-moving vehicle; **3) Queuing**, with the crowd forming a neat, orderly line; **4) Encircling**, involving the crowd gathers around an interesting object; **5) Passing**, with the crowd making temporary adjustments to navigate around a disturbance before resuming original activities; **6) Random**, characterized by the absence of clear collective movement. Leveraging GPT-4’s capabilities and embedded crowd knowledge, our planner selects an appropriate crowd response pattern to  $P_t$ , updates the current motions for affected individuals, and applies path change algorithms based on the response pattern to adjust their positions, as illustrated in Figure 3 (a).

**Microscopic Control.** Multi-person close interactions in crowd scenes require a more refined control mechanism. Given a scene context  $\mathcal{T}_{scene}$ , the planner  $\mathcal{P}$  is prompted to orchestrate the crowd’s movements. Utilizing a tree of thought approach, the planner  $\mathcal{P}$  systematically structures the scene setup in two stages: **(1) Scene Level:** Initially, the planner generates all potential motions applicable to the context  $\mathcal{T}_{scene}$ . Each motion is represented as a tuple  $(motion, possibility, interaction\_intensity, number\_of\_participants)$ , detailing the motion type, its likelihood of occurrence, the intensity of interaction, and the required number of participants. Leveraging predefined scene parameters  $\mathcal{C}_{params}$ , the planner then selects an appropriate set of final motions  $\mathcal{M}$  specific to the context  $\mathcal{T}_{scene}$ .

**(2) Group Level:** For each motion in  $\mathcal{M}$ , the planner  $\mathcal{P}$  establishes keyframes and issues comprehensive semantic and spatial plans for each individual’s motions, positions, and joint interactions. These plans encompass detailed textual descriptions of motions, quantified positions for movement, and specified distances between individuals’ joints. Finally, the planner  $\mathcal{P}$  efficiently coordinates these various interaction groups into logically positioned segments, considering their participant numbers and spatial requirements, as shown in Figure 3 (b).

**Unified Format.** To facilitate seamless integration with the motion generation process, we standardize control signals from both modes into semantic and spatial components as  $\mathcal{C}_{plan} = (\mathcal{C}^s, \mathcal{C}^t)$ . Semantic signals consist of textual motion descriptions, whereas spatial signals manage individual trajectories and joint positions at specific frames, as shown in Figure 2.

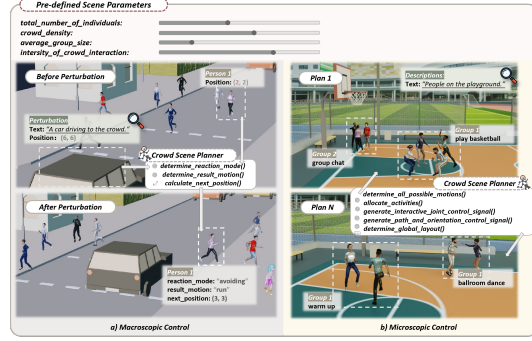


Figure 3: **Macro and Micro Control.** The **Crowd Scene Planner** is able to deal with crowd motions effectively at both the scene and motion levels. It manages both macroscopic crowd dynamics and microscopic detailed individual interactions, ensuring realistic and coherent crowd scenarios.

### 3.3 Collective Motion Generator

To enhance spatial controllability, previous works [59, 61] utilize ControlNet [67] to achieve spatial control. However, we argue that ControlNet does not consider the properties of motion representation, leading to unsatisfactory controllability. *First*, the spatial control signals in motion generation are more precise than that in image generation. The synthesized trajectory should be as same as the given signal, leading to a different optimal architecture design. *Second*, the spatial control signal is given in the joint-specific format. Thus, introducing the concept of joint-independent modeling is beneficial to capture features from spatial control signals. In our proposed **CrowdMoGen**, a diffusion model-based motion generation model, we carefully design **1) InputMixing** technique to effectively inject  $c^s$  into the input noised sequence  $\mathbf{x}_t$  within a joint-wise manner, **2) ControlAttention** module to adaptively refine motion feature based on the given spatial control signals and **3) training objectives** that drive the model to better align with the given control.

**Motion Diffusion Model.** Following approaches like MDM [57] and FineMoGen [71], we establish our network based on the off-the-shelf diffusion model [18]. A transformer-based backbone is applied to recover the clean motion sequence  $S(\mathbf{x}_t, t, c = \{c^t, c^s\})$  from noised sequence  $\mathbf{x}_t$ , with additional textual control signal  $c^t$  and spatial control signal  $c^s$ . The raw noised motion sequence  $\mathbf{x}_t$  and provided spatial control signal  $c^s$  are first processed by our proposed **InputMixing** technique. The mixed motion features are then passed by several transformer layers. Similar to the designs in the literature [69, 6], each layer includes an attention module, an FFN module, and stylization blocks.

**InputMixing.** During training,  $c^s \in \mathbb{R}^{F \times J \times 3}$  and a spatial control mask  $M_i \in \{0, 1\}^{F \times J}$  are provided to indicate the 3D trajectory of the controlled keypoints, where  $F$  denotes the number of frames and  $J$  represents the number of joints. To extract joint-wise information, we introduce two joint-wise encoder sets  $\{E_j^s\}, \{E_j^m\}$ . The output is formatted as  $s_{i,j} = M_{i,j} E_j^s(c_{i,j}^s) + (1 - M_{i,j}) c_{i,j}^{temp} + E_j^m((\mathbf{x}_t)_{i,j})$  for each frame  $i$  and each joint  $j$ , where  $c^{temp} \in \mathbb{R}^{F \times J \times L}$  is the learnable joint template, ensuring that both controlled and uncontrolled joints are accounted for in a rational manner.  $L$  is the dimension of latent feature for each joint.

Table 1: **Controllable motion generation quantitative results on HumanML3D test set.** ‘↑’(‘↓’) indicates that the values are better if the metric is larger (smaller). ‘→’ means closer to real data is better. The best result are in **bold**.

| Method                 | Joint        | FID ↓        | R-precision (Top-3) ↑ | Diversity →  | Foot skating ratio ↓ | Traj. err. (50 cm) ↓ | Loc. err. (50 cm) ↓ | Avg. err. (m) ↓ |
|------------------------|--------------|--------------|-----------------------|--------------|----------------------|----------------------|---------------------|-----------------|
| Real                   |              | 0.002        | 0.797                 | 9.503        | 0.000                | 0.000                | 0.000               | 0.000           |
| PriorMDM [48]          | Pelvis       | 0.475        | 0.583                 | 9.156        | 0.0897               | 0.3457               | 0.2132              | 0.4417          |
| GMD [23]               |              | 0.576        | 0.665                 | 9.206        | 0.109                | 0.0931               | 0.0321              | 0.1439          |
| OmniControl [61]       |              | 0.218        | 0.687                 | 9.422        | <b>0.0547</b>        | 0.0387               | 0.0096              | 0.0338          |
| InterControl [59]      |              | 0.159        | 0.671                 | <b>9.482</b> | 0.0729               | 0.0132               | 0.0004              | 0.0496          |
| <i>Ours CrowdMoGen</i> |              | <b>0.132</b> | <b>0.784</b>          | 9.109        | 0.0762               | <b>0.0000</b>        | <b>0.0000</b>       | <b>0.0196</b>   |
| OmniControl [61]       | Random One   | 0.310        | 0.693                 | <b>9.502</b> | <b>0.0608</b>        | 0.0617               | 0.0107              | 0.0404          |
| InterControl [59]      |              | 0.178        | 0.669                 | 9.498        | 0.0968               | 0.0403               | 0.0031              | 0.0741          |
| <i>Ours CrowdMoGen</i> |              | <b>0.147</b> | <b>0.781</b>          | 9.461        | 0.0829               | <b>0.0000</b>        | <b>0.0000</b>       | <b>0.0028</b>   |
| InterControl [59]      | Random Two   | 0.184        | 0.670                 | <b>9.410</b> | 0.0948               | 0.0475               | 0.0030              | 0.0911          |
| <i>Ours CrowdMoGen</i> |              | <b>0.178</b> | <b>0.777</b>          | 9.149        | <b>0.0865</b>        | <b>0.0000</b>        | <b>0.0000</b>       | <b>0.0027</b>   |
| InterControl [59]      | Random Three | 0.199        | 0.673                 | <b>9.352</b> | 0.0930               | 0.0487               | 0.0026              | 0.0969          |
| <i>Ours CrowdMoGen</i> |              | <b>0.192</b> | <b>0.778</b>          | 9.169        | <b>0.0871</b>        | <b>0.0000</b>        | <b>0.0000</b>       | <b>0.0030</b>   |

**ControlAttention.** Efficient Attention [49, 68] module and its variants SMA [69], DSMA [6] and SAMI [71] can aggregate global information effectively, enhancing semantic understanding of motion sequences beyond classical self-attention mechanisms. However, its focus on global information often complicates the realization of sparse and dynamic spatial control. The pattern of spatial control signal is critical but ignored in these designs. To address this, we upgrade the architecture of Efficient Attention and introduce a new attention mechanism *ControlAttention*. Specifically, we have two modifications: *First*, consider the nature of multi-head attention mechanism and our needs for joint-wise modelling, we set the number of attention heads to be same as the number of joints  $J$ . Thus, each head can focus more on the corresponding joint and better utilize the given joint-specific control signal; *Second*, *ControlAttention* incorporates additional learnable spatial embeddings into the attention mechanism to better capture spatial guidance. We define these embeddings for the Query  $\mathbf{Q}$  and Value  $\mathbf{V}$  vectors as follows:

$$\begin{aligned} emb_Q &= emb_Q^{mask} M + emb_Q^{control} (1 - M), \\ emb_V &= emb_V^{mask} M + emb_V^{control} (1 - M). \end{aligned} \quad (1)$$

In this formulation,  $emb_Q^{mask} \in \mathbb{R}^{F,J,L}$  and  $emb_V^{mask} \in \mathbb{R}^{F,J,L}$  are used to learn and integrate spatial information from uncontrolled joints, whereas  $emb_Q^{control}$  and  $emb_V^{control}$  focus on controlled joints. Therefore, the combined embeddings  $emb_Q$  and  $emb_V$  encapsulate comprehensive spatial details for both active and inactive joints, and are then added to the module input and utilized for computing the  $Q$  and  $V$  vectors. Our *ControlAttention* thus enhances the model’s ability to manage joint status flexibly and accurately.

**Training Objectives.** During training, our method diverges from traditional approaches [61, 59] that typically compute the mean square error (MSE) solely based on the whole body motion  $\hat{x}_0$ , presented in a relative motion format. To enhance motion precision and the naturalness of the animations, we extend the commonly used *Whole Body Loss*  $\mathcal{L}_{whole}$  by incorporating two additional loss components: *Controlled Keypoint Loss*  $\mathcal{L}_{con}$  and *Foot Skating Loss*  $\mathcal{L}_{foot}$ . The *Controlled Keypoint Loss* computes the 3-dimensional Euclidean distance between controlled keypoints and their corresponding global signals. The *Foot Skating Loss* assesses the sliding of the foot joint, supervising the 3-dimensional Euclidean distance between the foot joints in two consecutive frames if their heights are below a certain threshold  $h_{\text{thresh}}$ . Specifically, we transform the output predictions  $\hat{x}_0 \in \mathbb{R}^{F \times D}$  into a global 3D keypoint representation  $\hat{x}_0^g \in \mathbb{R}^{F \times J \times 3}$ . We then compute the *Controlled Keypoint Loss*  $\mathcal{L}_{con}$  and *Foot Skating Loss*  $\mathcal{L}_{foot}$  as follows:

$$\mathcal{L}_{con} = M \|c^s - \hat{x}_0^g\|_2, \mathcal{L}_{foot} = \sum_{i=1}^{F-1} \left( \sum_{j \in \{j_{\text{left}}, j_{\text{right}}\}} \left( (\hat{x}_0^g)_{i,j,2} < h_{\text{thresh}} \right) \cdot \left\| (\hat{x}_0^g)_{i+1,j} - (\hat{x}_0^g)_{i,j} \right\|_2 \right). \quad (2)$$

Here,  $M \in \mathbb{R}^{F \times D}$  aggregates all  $M_i$ , representing the control status across the entire motion sequence. The indices  $j_{\text{left}}$  and  $j_{\text{right}}$  denote the left and right foot keypoints, respectively. The overall training objectives can be formulated as:

$$\mathcal{L} = \lambda_{\text{whole}} \cdot \mathcal{L}_{\text{whole}} + \lambda_{\text{con}} \cdot \mathcal{L}_{\text{con}} + \lambda_{\text{foot}} \cdot \mathcal{L}_{\text{foot}}, \quad (3)$$

Table 2: **Text-to-motion evaluation on KIL-ML test set.** ‘↑’(‘↓’) indicates that the values are better if the metric is larger (smaller). ‘→’ means closer to real data is better. The best results are in **bold**.

| Method                 | FID ↓        | R-precision (Top-3) ↑ | Diversity →  |
|------------------------|--------------|-----------------------|--------------|
| Real                   | 0.031        | 0.779                 | 11.08        |
| T2M [14]               | 3.022        | 0.681                 | 10.72        |
| MotionDiffuse [68]     | 1.954        | 0.739                 | <b>11.10</b> |
| MLD [8]                | 0.404        | 0.734                 | 10.80        |
| T2M-GPT [66]           | 0.514        | 0.745                 | 10.92        |
| MotionGPT [21]         | 0.510        | 0.680                 | 10.35        |
| MDM [57]               | 0.497        | 0.396                 | 10.84        |
| PriorMDM [48]          | 0.830        | 0.397                 | 10.54        |
| GMD [23]               | 1.537        | 0.385                 | 9.78         |
| OmniControl [61]       | 0.702        | 0.397                 | 10.93        |
| InterControl [59]      | 0.580        | 0.397                 | 10.88        |
| <i>Ours CrowdMoGen</i> | <b>0.217</b> | <b>0.777</b>          | 10.33        |

Table 3: **Text-to-motion evaluation on HumanML3D test set.** The best results are in **bold**.

| Method                 | FID ↓        | R-precision (Top-3) ↑ | Diversity →  |
|------------------------|--------------|-----------------------|--------------|
| Real                   | 0.002        | 0.797                 | 9.503        |
| T2M [14]               | 1.067        | 0.740                 | 9.188        |
| MotionDiffuse [68]     | 0.630        | 0.782                 | 9.410        |
| MLD [8]                | 0.473        | 0.772                 | 9.724        |
| PhysDiff [65]          | 0.413        | 0.631                 | -            |
| T2M-GPT [66]           | <b>0.116</b> | 0.775                 | 9.761        |
| MotionGPT [21]         | 0.232        | 0.778                 | 9.528        |
| MDM [57]               | 0.544        | 0.611                 | 9.446        |
| PriorMDM [48]          | 0.540        | 0.640                 | 9.160        |
| GMD [23]               | 0.212        | 0.670                 | 9.440        |
| OmniControl [61]       | 0.218        | 0.687                 | 9.422        |
| InterControl [59]      | 0.159        | 0.671                 | <b>9.482</b> |
| <i>Ours CrowdMoGen</i> | 0.132        | <b>0.784</b>          | 9.109        |

where  $\lambda_{whole}, \lambda_{con}, \lambda_{foot}$  are hyper-parameters.

**Inference Strategies.** During inference stage, we apply a 50-step denoising process to synthesize motion sequences while using classifier-free guidance for better generation quality. In addition, we use IK guidance [59] in the last iterations for better spatial alignment.

## 4 Experiments

### 4.1 Datasets and Metrics

**Datasets.** We conduct experiments on the HumanML3D [14] and KIT-ML [45] datasets to evaluate the generation and control capabilities of the proposed **Collective Motion Generator**. The HumanML3D dataset, a reannotated combination of the HumanAct12 [15] and AMASS [36] datasets, comprises 14,616 motions and 44,970 textual descriptions. The KIT Motion Language Dataset includes 3,911 motions accompanied by 6,363 natural language descriptions.

**Evaluation Metrics.** Following [14], we use *Frechet Inception Distance (FID)*, *R-Precision*, and *Diversity* to evaluate the quality of generated motions, similarity to the textual descriptions, and generation variability, respectively. Following OmniControl [61], we employ *Foot Skating Ratio*, *Trajectory Error*, *Location Error*, and *Average Error* to evaluate the control accuracy of the proposed **Collective Motion Generator**.

### 4.2 Implementation Details

We construct a 4-layer transformer as the motion decoder. For the text encoder, we initially use the CLIP ViT-B/32 text encoder and then add two additional transformer encoder layers. Both the text encoder and the motion decoder have a latent dimension of 512.  $\lambda_{whole}, \lambda_{con}, \lambda_{foot}$  are all set to 1.0. The diffusion model employs 1000 diffusion steps, with variances  $\beta_t$  linearly ranging from 0.0001 to 0.02. Training is conducted on eight Tesla V100 GPUs, each processing 64 samples, resulting in a total batch size of 512. The total number of iterations is around 40,000 for KIT-ML and 100,000 for HumanML3D. We utilize the Adam optimizer to train the model with an initial learning rate of  $2e^{-4}$  and decrease it to  $2e^{-5}$  in the last 20% iterations.

### 4.3 Quantitative Results

Table 1 shows the quantitative comparison about spatial controllability. Our **Collective Motion Generator** (CMG) has better motion quality (FID), text-motion consistency (R-precision), and spatial error. We also want to highlight that the trajectory of our generated motion sequences are almost as same as the given spatial condition. These results demonstrate CMG’s ability to produce realistic and text-aligned motion sequences that meet specific spatial conditions. In addition, we compare

Table 4: **Ablation studies on the HumanML3D dataset.** ‘↑’(‘↓’) indicates that the values are better if the metric is larger (smaller). ‘→’ means closer to real data is better. The best results are in **bold**.

| Item | Method               | FID ↓        | R-precision (Top-3) ↑ | Diversity →  | Foot skating ratio ↓ | Traj. err. (20 cm) ↓ | Loc. err. (20 cm) ↓ | Avg. err. (m) ↓ |
|------|----------------------|--------------|-----------------------|--------------|----------------------|----------------------|---------------------|-----------------|
| (1)  | <b>CrowdMoGen</b>    | 0.132        | <b>0.784</b>          | 9.109        | 0.0762               | <b>0.0051</b>        | <b>0.0000</b>       | 0.0196          |
| (2)  | w/o ControlAttention | 0.150        | 0.775                 | <b>9.446</b> | 0.1037               | 0.0069               | 0.0001              | 0.0223          |
| (3)  | w/o InputMixing      | 0.207        | 0.771                 | 9.090        | 0.0919               | 0.0159               | 0.0003              | 0.0246          |
| (4)  | w/o Joint Loss       | 0.219        | 0.761                 | 9.143        | 0.1316               | 0.0174               | 0.0004              | 0.0254          |
| (5)  | w/o Skating Loss     | <b>0.125</b> | 0.777                 | 9.244        | 0.1947               | 0.0058               | 0.0001              | <b>0.0147</b>   |
| (6)  | w/o IK guidance      | 0.130        | 0.782                 | 9.320        | <b>0.0751</b>        | 0.5710               | 0.2720              | 0.2387          |
| (7)  | ControlNet           | 0.225        | 0.763                 | 9.814        | 0.0915               | 0.0210               | 0.0005              | 0.0427          |

our generated results to existing text-to-motion methods and find that CMG performs competitively, despite not being specifically designed for this task (see Tables 2 and 3).

**User Study.** Considering the challenges in evaluating text consistency and crowd motion quality, we conducted a user study to assess Crowd Scene Planner. We invited 50 participants, including animators, AI researchers, and gaming enthusiasts, aged 20 to 35. They were provided with textual descriptions and asked to compare crowd motions planned by our module versus those generated by the original GPT-4, focusing on motion quality and text consistency. The original GPT-4, without specialized prompt engineering, struggles to accurately integrate joint interactions, global paths, and overall planning. In contrast, our module employs a sophisticated tree-of-thought approach that divides planning into macro and micro levels, effectively addressing the challenges of semantic and spatial integration that GPT-4 faces. As shown in Figure 4, our user study validates the superior performance of our planner in producing coherent and contextually accurate crowd motion plans.



Figure 4: **User Study: Comparative Analysis of Planning Methods.** This chart presents the comparison results between our **Crowd Scene Planner** and plain GPT-4, based on participant preferences for text-motion consistency (TM. Con.) and motion quality (M. Qual.). The percentages reflect the proportion of participants who favored each method.

#### 4.4 Qualitative Results

**Crowd Motion Generation.** As shown in Figure 5 (a)-(f), we randomly generated three groups of crowd motions involving multi-person close interactions (a)-(b), larger-scale crowd dynamics under given perturbations (c)-(d), and complex crowd scene arrangements (e)-(f) using **CrowdMoGen**. The generated crowd’s have natural and reasonable motion semantics, realistic dynamics, as well as accurate joint interactions. This illustrate that our proposed method excels at both macro and micro-level control and generation for crowd motions.

#### 4.5 Ablation Study

We present the ablation results in Table 4. Although IK guidance is essential for satisfying spatial alignment as shown in Experiment (6), the architecture design and loss design are also indispensable. For example, in Experiment (7), we attempt to use only the ControlNet structure and IK guidance. The results show significantly poorer motion quality and spatial consistency compared to our final CrowdMoGen algorithm, which strongly prove the necessity of our proposed components. Experiments (1)(2)(3) demonstrate that our proposed architectural design effectively incorporates the given spatial signal into the motion transformer, enabling the model to generate high-quality motion sequences that are consistent with the provided textual description and spatial control signals simultaneously. The effectiveness of loss design are also proved in Experiments (1)(4)(5), which mainly ameliorates the keypoint error and foot skating ratio respectively.

#### 4.6 Limitations and Potential Societal Impacts

**Limitations.** Our **Crowd Scene Planner** depends on the capabilities of the Large Language Model (LLM), which may not always accurately predict complex or rare crowd scenarios. Additionally,



Figure 5: **Qualitative Visualizations.** Displayed are selected frames from the crowd motion sequences generated by our proposed **CrowdMoGen**. It effectively creates scenarios involving multi-person close interactions (a)-(b), dynamic crowd movements (c)-(d), and complex crowd scenes (e)-(f) that accurately and naturally reflect the specified scene descriptions.

the **Collective Motion Generator** may experience conflicts from multiple control signals. These challenges highlight the need for further enhancements in modeling crowd dynamics.

**Potential Social Impacts.** The proposed **CrowdMoGen** may offer significant benefits by enhancing realism and interactivity in virtual environments for entertainment and urban planning. However, it can also be misused to fabricate deceptive crowd scenes for simulations or entertainment, potentially misrepresenting public events or influencing opinions.

## 5 Conclusion

In this work, we introduce and explore the novel task of *Crowd Motion Generation*, aimed at realistically producing collective human motions tailored to specific scene settings. Moreover, we also propose **CrowdMoGen**, a groundbreaking, zero-shot, text-driven framework for crowd motion generation. This framework utilizes the off-the-shelf Large Language Model alongside a carefully designed motion generation model that allows for fine-grained spatial and semantic control, enabling the autonomous and efficient generation of versatile crowd dynamics. Our innovative approach provides fresh insights into human motion generation and would be a good inspiration for future developments in various industries such as animation, gaming, and urban planning.

## 6 Acknowledgment

This study is supported by the Ministry of Education, Singapore, under its MOE AcRF Tier 2 (MOET2EP20221- 0012), NTU NAP, and under the RIE2020 Industry Alignment Fund– Industry Collaboration Projects (IAF-ICP) Funding Initiative, as well as cash and in-kind contribution from the industry partner(s).

## References

- [1] Hyemin Ahn and Dongheui Mascaro, Valls Esteve and Lee. Can we use diffusion probabilistic models for 3d motion prediction? In *2023 IEEE International Conference on Robotics and Automation (ICRA)*, May 2023.
- [2] Hyemin Ahn, Esteve Valls Mascaro, and Dongheui Lee. Can we use diffusion probabilistic models for 3d motion prediction? *arXiv preprint arXiv:2302.14503*, 2023.
- [3] Nikos Athanasiou, Mathis Petrovich, Michael J Black, and Gül Varol. Teach: Temporal action composition for 3d humans. In *2022 International Conference on 3D Vision (3DV)*, pages 414–423. IEEE, 2022.
- [4] German Barquero, Sergio Escalera, and Cristina Palmero. Belfusion: Latent diffusion for behavior-driven human motion prediction. In *Proceedings of the IEEE/CVF International Conference on Computer Vision*, pages 2317–2327, 2023.
- [5] Emad Barsoum, John Kender, and Zicheng Liu. Hp-gan: Probabilistic 3d human motion prediction via gan. In *Proceedings of the IEEE conference on computer vision and pattern recognition workshops*, pages 1418–1427, 2018.
- [6] Zhongang Cai, Jianping Jiang, Zhongfei Qing, Xinying Guo, Mingyuan Zhang, Zhengyu Lin, Haiyi Mei, Chen Wei, Ruisi Wang, Wanqi Yin, et al. Digital life project: Autonomous 3d characters with social intelligence. *arXiv preprint arXiv:2312.04547*, 2023.
- [7] Ling-Hao Chen, Jiawei Zhang, Yewen Li, Yiren Pang, Xiaobo Xia, and Tongliang Liu. Human-mac: Masked motion completion for human motion prediction. 2023.
- [8] Xin Chen, Biao Jiang, Wen Liu, Zilong Huang, Bin Fu, Tao Chen, and Gang Yu. Executing your commands via motion diffusion in latent space. In *Proceedings of the IEEE/CVF Conference on Computer Vision and Pattern Recognition*, pages 18000–18010, 2023.
- [9] Baptiste Chopin, Hao Tang, and Mohamed Daoudi. Bipartite graph diffusion model for human interaction generation. In *Proceedings of the IEEE/CVF Winter Conference on Applications of Computer Vision*, pages 5333–5342, 2024.
- [10] Christian Diller and Angela Dai. Cg-hoi: Contact-guided 3d human-object interaction generation. *arXiv preprint arXiv:2311.16097*, 2023.
- [11] Christian Diller, Thomas Funkhouser, and Angela Dai. Forecasting characteristic 3d poses of human actions. 2022.
- [12] Kehong Gong, Dongze Lian, Heng Chang, Chuan Guo, Zihang Jiang, Xinxin Zuo, Michael Bi Mi, and Xinchao Wang. Tm2d: Bimodality driven 3d dance generation via music-text integration. In *Proceedings of the IEEE/CVF International Conference on Computer Vision*, pages 9942–9952, 2023.
- [13] Anand Gopalakrishnan, Ankur Mali, Dan Kifer, Lee Giles, and Alexander G Ororbia. A neural temporal model for human motion prediction. In *Proceedings of the IEEE/CVF Conference on Computer Vision and Pattern Recognition*, pages 12116–12125, 2019.
- [14] Chuan Guo, Shihao Zou, Xinxin Zuo, Sen Wang, Wei Ji, Xingyu Li, and Li Cheng. Generating diverse and natural 3d human motions from text. In *Proceedings of the IEEE/CVF Conference on Computer Vision and Pattern Recognition*, pages 5152–5161, 2022.
- [15] Chuan Guo, Xinxin Zuo, Sen Wang, Shihao Zou, Qingyao Sun, Annan Deng, Minglun Gong, and Li Cheng. Action2motion: Conditioned generation of 3d human motions. In *Proceedings of the 28th ACM International Conference on Multimedia*, pages 2021–2029, 2020.
- [16] Wen Guo, Yuming Du, Xi Shen, Vincent Lepetit, Xavier Alameda-Pineda, and Francesc Moreno-Noguer. Back to mlp: A simple baseline for human motion prediction. In *Proceedings of the IEEE/CVF Winter Conference on Applications of Computer Vision*, pages 4809–4819, 2023.
- [17] Yuze Hao, Jianrong Zhang, Tao Zhuo, Fuan Wen, and Hehe Fan. Hand-centric motion refinement for 3d hand-object interaction via hierarchical spatial-temporal modeling. *arXiv preprint arXiv:2401.15987*, 2024.
- [18] Jonathan Ho, Ajay Jain, and Pieter Abbeel. Denoising diffusion probabilistic models. *Advances in Neural Information Processing Systems*, 33:6840–6851, 2020.

- [19] Nhat M Hoang, Kehong Gong, Chuan Guo, and Michael Bi Mi. Motionmix: Weakly-supervised diffusion for controllable motion generation. *arXiv preprint arXiv:2401.11115*, 2024.
- [20] Siyuan Huang, Zan Wang, Puhao Li, Baoxiong Jia, Tengyu Liu, Yixin Zhu, Wei Liang, and Song-Chun Zhu. Diffusion-based generation, optimization, and planning in 3d scenes. In *Proceedings of the IEEE/CVF Conference on Computer Vision and Pattern Recognition*, pages 16750–16761, 2023.
- [21] Biao Jiang, Xin Chen, Wen Liu, Jingyi Yu, Gang Yu, and Tao Chen. Motiongpt: Human motion as a foreign language. *Advances in Neural Information Processing Systems*, 36, 2024.
- [22] Chiyu Jiang, Andre Cornman, Cheolho Park, Benjamin Sapp, Yin Zhou, Dragomir Anguelov, et al. Motiondiffuser: Controllable multi-agent motion prediction using diffusion. In *Proceedings of the IEEE/CVF Conference on Computer Vision and Pattern Recognition*, pages 9644–9653, 2023.
- [23] Korrawe Karunratanakul, Konpat Preechakul, Supasorn Suwajanakorn, and Siyu Tang. Guided motion diffusion for controllable human motion synthesis. In *Proceedings of the IEEE/CVF International Conference on Computer Vision*, pages 2151–2162, 2023.
- [24] Jihoon Kim, Jiseob Kim, and Sungjoon Choi. Flame: Free-form language-based motion synthesis & editing. In *Proceedings of the AAAI Conference on Artificial Intelligence*, volume 37, pages 8255–8263, 2023.
- [25] Sumith Kulal, Jiayuan Mao, Alex Aiken, and Jiajun Wu. Programmatic concept learning for human motion description and synthesis. In *Proceedings of the IEEE/CVF Conference on Computer Vision and Pattern Recognition*, pages 13843–13852, 2022.
- [26] Jiaman Li, Alexander Clegg, Roozbeh Mottaghi, Jiajun Wu, Xavier Puig, and C Karen Liu. Controllable human-object interaction synthesis. *arXiv preprint arXiv:2312.03913*, 2023.
- [27] Ruilong Li, Shan Yang, David A Ross, and Angjoo Kanazawa. Ai choreographer: Music conditioned 3d dance generation with aist++. In *Proceedings of the IEEE/CVF International Conference on Computer Vision*, pages 13401–13412, 2021.
- [28] Han Liang, Wenqian Zhang, Wenxuan Li, Jingyi Yu, and Lan Xu. Intergen: Diffusion-based multi-human motion generation under complex interactions. *arXiv preprint arXiv:2304.05684*, 2023.
- [29] Donggeun Lim, Cheongi Jeong, and Young Min Kim. Mammos: Mapping multiple human motion with scene understanding and natural interactions. In *Proceedings of the IEEE/CVF International Conference on Computer Vision*, pages 4278–4287, 2023.
- [30] Junfan Lin, Jianlong Chang, Lingbo Liu, Guanbin Li, Liang Lin, Qi Tian, and Chang-wen Chen. Ohmg: Zero-shot open-vocabulary human motion generation. *arXiv preprint arXiv:2210.15929*, 2022.
- [31] Pei Lin, Sihang Xu, Hongdi Yang, Yiran Liu, Xin Chen, Jingya Wang, Jingyi Yu, and Lan Xu. Handdiffuse: Generative controllers for two-hand interactions via diffusion models. *arXiv preprint arXiv:2312.04867*, 2023.
- [32] Jun Liu, Amir Shahroudy, Mauricio Perez, Gang Wang, Ling-Yu Duan, and Alex C Kot. Ntu rgb+ d 120: A large-scale benchmark for 3d human activity understanding. *IEEE transactions on pattern analysis and machine intelligence*, 42(10):2684–2701, 2019.
- [33] Xinpeng Liu, Haowen Hou, Yanchao Yang, Yong-Lu Li, and Cewu Lu. Revisit human-scene interaction via space occupancy. *arXiv preprint arXiv:2312.02700*, 2023.
- [34] Yunhong Lou, Linchao Zhu, Yaxiong Wang, Xiaohan Wang, and Yi Yang. Diversemotion: Towards diverse human motion generation via discrete diffusion. *arXiv preprint arXiv:2309.01372*, 2023.
- [35] Shunlin Lu, Ling-Hao Chen, Ailing Zeng, Jing Lin, Ruimao Zhang, Lei Zhang, and Heung-Yeung Shum. Humantomato: Text-aligned whole-body motion generation. *arXiv preprint arXiv:2310.12978*, 2023.
- [36] Naureen Mahmood, Nima Ghorbani, Nikolaus F Troje, Gerard Pons-Moll, and Michael J Black. Amass: Archive of motion capture as surface shapes. In *Proceedings of the IEEE/CVF International Conference on Computer Vision*, pages 5442–5451, 2019.

- [37] Wei Mao, Miaomiao Liu, and Mathieu Salzmann. History repeats itself: Human motion prediction via motion attention. In *Computer Vision—ECCV 2020: 16th European Conference, Glasgow, UK, August 23–28, 2020, Proceedings, Part XIV 16*, pages 474–489. Springer, 2020.
- [38] Dushyant Mehta, Helge Rhodin, Dan Casas, Pascal Fua, Oleksandr Sotnychenko, Weipeng Xu, and Christian Theobalt. Monocular 3d human pose estimation in the wild using improved cnn supervision. In *3D Vision (3DV), 2017 Fifth International Conference on*. IEEE, 2017.
- [39] Miki Okamura, Naruya Kondo, Tatsuki Fushimi Maki Sakamoto, and Yoichi Ochiai. Dance generation by sound symbolic words. *arXiv preprint arXiv:2306.03646*, 2023.
- [40] Xiaogang Peng, Yiming Xie, Zizhao Wu, Varun Jampani, Deqing Sun, and Huaizu Jiang. Hoi-diff: Text-driven synthesis of 3d human-object interactions using diffusion models. *arXiv preprint arXiv:2312.06553*, 2023.
- [41] Mathis Petrovich, Michael J Black, and Gül Varol. Action-conditioned 3d human motion synthesis with transformer vae. In *Proceedings of the IEEE/CVF International Conference on Computer Vision*, pages 10985–10995, 2021.
- [42] Mathis Petrovich, Michael J Black, and Gül Varol. Temos: Generating diverse human motions from textual descriptions. In *European Conference on Computer Vision*, pages 480–497. Springer, 2022.
- [43] Mathis Petrovich, Or Litany, Umar Iqbal, Michael J Black, Gül Varol, Xue Bin Peng, and Davis Rempe. Multi-track timeline control for text-driven 3d human motion generation. *arXiv preprint arXiv:2401.08559*, 2024.
- [44] Huaijin Pi, Sida Peng, Minghui Yang, Xiaowei Zhou, and Hujun Bao. Hierarchical generation of human-object interactions with diffusion probabilistic models. In *Proceedings of the IEEE/CVF International Conference on Computer Vision*, pages 15061–15073, 2023.
- [45] Matthias Plappert, Christian Mandery, and Tamim Asfour. The kit motion-language dataset. *Big data*, 4(4):236–252, 2016.
- [46] Davis Rempe, Zhengyi Luo, Xue Bin Peng, Ye Yuan, Kris Kitani, Karsten Kreis, Sanja Fidler, and Or Litany. Trace and pace: Controllable pedestrian animation via guided trajectory diffusion. In *Conference on Computer Vision and Pattern Recognition (CVPR)*, 2023.
- [47] Jiawei Ren, Mingyuan Zhang, Cunjun Yu, Xiao Ma, Liang Pan, and Ziwei Liu. Insactor: Instruction-driven physics-based characters. *Advances in Neural Information Processing Systems*, 36, 2024.
- [48] Yonatan Shafir, Guy Tevet, Roy Kapon, and Amit H Bermano. Human motion diffusion as a generative prior. *arXiv preprint arXiv:2303.01418*, 2023.
- [49] Zhuoran Shen, Mingyuan Zhang, Haiyu Zhao, Shuai Yi, and Hongsheng Li. Efficient attention: Attention with linear complexities. In *Proceedings of the IEEE/CVF winter conference on applications of computer vision*, pages 3531–3539, 2021.
- [50] Xu Shi, Chuanchen Luo, Junran Peng, Hongwen Zhang, and Yunlian Sun. Generating fine-grained human motions using chatgpt-refined descriptions. *arXiv preprint arXiv:2312.02772*, 2023.
- [51] Soshi Shimada, Franziska Mueller, Jan Bednarik, Bardia Doosti, Bernd Bickel, Danhang Tang, Vladislav Golyanik, Jonathan Taylor, Christian Theobalt, and Thabo Beeler. Macs: Mass conditioned 3d hand and object motion synthesis. *arXiv preprint arXiv:2312.14929*, 2023.
- [52] Li Siyao, Weijiang Yu, Tianpei Gu, Chunze Lin, Quan Wang, Chen Qian, Chen Change Loy, and Ziwei Liu. Bailando: 3d dance generation by actor-critic gpt with choreographic memory. In *Proceedings of the IEEE/CVF Conference on Computer Vision and Pattern Recognition*, pages 11050–11059, 2022.
- [53] Jiangxin Sun, Zihang Lin, Xintong Han, Jian-Fang Hu, Jia Xu, and Wei-Shi Zheng. Action-guided 3d human motion prediction. *Advances in Neural Information Processing Systems*, 34:30169–30180, 2021.
- [54] Jiarui Sun and Girish Chowdhary. Towards globally consistent stochastic human motion prediction via motion diffusion. *arXiv preprint arXiv:2305.12554*, 2023.
- [55] Purva Tendulkar, Dídac Surís, and Carl Vondrick. Flex: Full-body grasping without full-body grasps. In *Proceedings of the IEEE/CVF Conference on Computer Vision and Pattern Recognition*, pages 21179–21189, 2023.

- [56] Guy Tevet, Brian Gordon, Amir Hertz, Amit H Bermano, and Daniel Cohen-Or. Motionclip: Exposing human motion generation to clip space. In *European Conference on Computer Vision*, pages 358–374. Springer, 2022.
- [57] Guy Tevet, Sigal Raab, Brian Gordon, Yoni Shafir, Daniel Cohen-or, and Amit Haim Bermano. Human motion diffusion model. In *The Eleventh International Conference on Learning Representations*, 2022.
- [58] Xinshun Wang, Qiongjie Cui, Chen Chen, and Mengyuan Liu. Gcnex: Towards the unity of graph convolutions for human motion prediction. *arXiv preprint arXiv:2312.11850*, 2023.
- [59] Zhenzhi Wang, Jingbo Wang, Yixuan Li, Dahua Lin, and Bo Dai. Intercontrol: Generate human motion interactions by controlling every joint, 2024.
- [60] Zeqi Xiao, Tai Wang, Jingbo Wang, Jinkun Cao, Wenwei Zhang, Bo Dai, Dahua Lin, and Jiangmiao Pang. Unified human-scene interaction via prompted chain-of-contacts. *arXiv preprint arXiv:2309.07918*, 2023.
- [61] Yiming Xie, Varun Jampani, Lei Zhong, Deqing Sun, and Huaizu Jiang. Omnicontrol: Control any joint at any time for human motion generation. *arXiv preprint arXiv:2310.08580*, 2023.
- [62] Haodong Yan, Zhiming Hu, Syn Schmitt, and Andreas Bulling. Gazemodiff: Gaze-guided diffusion model for stochastic human motion prediction. *arXiv preprint arXiv:2312.12090*, 2023.
- [63] Siyue Yao, Mingjie Sun, Bingliang Li, Fengyu Yang, Junle Wang, and Ruimao Zhang. Dance with you: The diversity controllable dancer generation via diffusion models. In *Proceedings of the 31st ACM International Conference on Multimedia*, pages 8504–8514, 2023.
- [64] Payam Jome Yazdian, Eric Liu, Li Cheng, and Angelica Lim. Motionscript: Natural language descriptions for expressive 3d human motions. *arXiv preprint arXiv:2312.12634*, 2023.
- [65] Ye Yuan, Jiaming Song, Umar Iqbal, Arash Vahdat, and Jan Kautz. Physdiff: Physics-guided human motion diffusion model. In *Proceedings of the IEEE/CVF International Conference on Computer Vision*, pages 16010–16021, 2023.
- [66] Jianrong Zhang, Yangsong Zhang, Xiaodong Cun, Shaoli Huang, Yong Zhang, Hongwei Zhao, Hongtao Lu, and Xi Shen. T2m-gpt: Generating human motion from textual descriptions with discrete representations. *arXiv preprint arXiv:2301.06052*, 2023.
- [67] Lvmin Zhang, Anyi Rao, and Maneesh Agrawala. Adding conditional control to text-to-image diffusion models, 2023.
- [68] Mingyuan Zhang, Zhongang Cai, Liang Pan, Fangzhou Hong, Xinying Guo, Lei Yang, and Ziwei Liu. Motiondiffuse: Text-driven human motion generation with diffusion model. *IEEE Transactions on Pattern Analysis and Machine Intelligence*, 2024.
- [69] Mingyuan Zhang, Xinying Guo, Liang Pan, Zhongang Cai, Fangzhou Hong, Huirong Li, Lei Yang, and Ziwei Liu. Remodiffuse: Retrieval-augmented motion diffusion model. In *IEEE/CVF International Conference on Computer Vision, ICCV 2023, Paris, France, October 1-6, 2023*, pages 364–373, 2023.
- [70] Mingyuan Zhang, Daisheng Jin, Chenyang Gu, Fangzhou Hong, Zhongang Cai, Jingfang Huang, Chongzhi Zhang, Xinying Guo, Lei Yang, Ying He, and Ziwei Liu. Large motion model for unified multi-modal motion generation, 2024.
- [71] Mingyuan Zhang, Huirong Li, Zhongang Cai, Jiawei Ren, Lei Yang, and Ziwei Liu. Finemogen: Fine-grained spatio-temporal motion generation and editing. *Advances in Neural Information Processing Systems*, 36, 2024.
- [72] Mengyi Zhao, Mengyuan Liu, Bin Ren, Shuling Dai, and Nicu Sebe. Modiff: Action-conditioned 3d motion generation with denoising diffusion probabilistic models. *arXiv preprint arXiv:2301.03949*, 2023.
- [73] Wentao Zhu, Jason Qin, Yuke Lou, Hang Ye, Xiaoxuan Ma, Hai Ci, and Yizhou Wang. Social motion prediction with cognitive hierarchies. In A. Oh, T. Naumann, A. Globerson, K. Saenko, M. Hardt, and S. Levine, editors, *Advances in Neural Information Processing Systems*, volume 36, pages 77675–77690. Curran Associates, Inc., 2023.
- [74] Wenlin Zhuang, Congyi Wang, Jinxiang Chai, Yangang Wang, Ming Shao, and Siyu Xia. Music2dance: Dancenet for music-driven dance generation. *ACM Transactions on Multimedia Computing, Communications, and Applications (TOMM)*, 18(2):1–21, 2022.

## A Details of CrowdMoGen

### A.1 Diffusion Model

Diffusion models can be defined using a Markov chain  $p_\theta(\mathbf{x}_0) := \int p_\theta(\mathbf{x}_{0:T}) d\mathbf{x}_{1:T}$ , where the intermediate variables  $\mathbf{x}_1, \dots, \mathbf{x}_T$  represent noised versions of the original data  $\mathbf{x}_0 \sim q(\mathbf{x}_0)$ , and maintains the same dimensionality as the original data. In motion generation, every  $\mathbf{x}_t$  corresponds to a motion sequence  $\theta_i \in \mathbb{R}^D, i = 1, 2, \dots, F$ , where  $D$  denotes the dimensionality of each pose, and  $F$  represents the total number of frames. In the diffusion process of diffusion models, [18] efficiently derive  $\mathbf{x}_t$  from  $x_0$  by approximating  $q(\mathbf{x}_t)$  as  $\mathbf{x} := \sqrt{\bar{\alpha}_t}\mathbf{x}_0 + \sqrt{1 - \bar{\alpha}_t}\epsilon$ , where  $\alpha_t := 1 - \beta_t$ ,  $\bar{\alpha}_t := \prod_{s=1}^t \alpha_s$ , and  $\beta_t$  is a predefined variance schedule at the  $t^{\text{th}}$  noising step. Then, the diffusion process is reversed for clean motion recovery. Specifically, a motion generation model  $S$  is configured to refine noisy data  $\mathbf{x}_t$  back to its original, clean state  $\mathbf{x}_0$ . Following approaches like MDM [57] and ReMoDiffuse [69], we estimate  $\mathbf{x}_0$  as  $S(\mathbf{x}_t, t, c)$ , where  $c$  represents the conditioning signal containing the spatial control signal  $c^s$  and the textual control signal  $c^t$ , and  $t \in \mathcal{U}(0, T)$  marks the timestep in the diffusion process. Finally in the sampling phase, we derive  $\mathbf{x}_{t-1}$  by sampling it from the Gaussian distribution  $\mathcal{N}(\mu_\theta(\mathbf{x}_t, t, c), \beta_t)$ , where the mean is specified as follows:

$$\begin{aligned} \mu_\theta(\mathbf{x}_t, t, c) &= \sqrt{\bar{\alpha}_t}S(\mathbf{x}_t, t, c) + \sqrt{1 - \bar{\alpha}_t}\epsilon_\theta(\mathbf{x}_t, t, c), \\ \epsilon_\theta(\mathbf{x}_t, t, c) &= \left(\frac{\mathbf{x}_t}{\sqrt{\bar{\alpha}_t}} - S(\mathbf{x}_t, t, c)\right)\sqrt{\frac{1}{\bar{\alpha}_t} - 1}. \end{aligned} \quad (4)$$

### A.2 Human Motion Representation

Human motion can be parameterized using two primary methods: relative or global joint representation. The relative representation, proposed in [14], is a redundant format that includes pelvis velocity, local joint positions, velocities, and rotations relative to the pelvis, complemented by foot contact binary labels. This representation method simplifies the model learning process and supports the generation of natural human motions aligning with inherent human body priors. However, it faces challenges in precise spatial control, especially in sparse time frames and when controlling joints beyond the pelvis, due to its lack of a stable global reference. Consequently, controlling methods [57, 23] using this format struggle with consistency and precision in joint-wise spatial control across timesteps. In contrast, global joint representation provides each joint’s absolute coordinates within a global framework, offering clear and direct reference for fine-grained control. Therefore, inspired by [61], we employ a hybrid approach to represent motions in our framework: utilizing relative representation for training and routine generation, and switching to global positioning for enhanced spatial control.

### A.3 IK Guidance

Noise optimization during the sampling stage enhances the spatial control capabilities of our model. In diffusion steps, gradient descent optimization is performed on the output mean in response to the input spatial control signals. Specifically,  $\mathcal{D}(\mu_\theta(\mathbf{x}_t, t, c), c^s)$  quantifies the discrepancy between the currently generated mean  $\mu_\theta(\mathbf{x}_t, t, c)$  and the provided spatial signal  $c^s$ . To ensure precise control, we can selectively supervise specific time frames and joints, while masking unsupervised components.

$$\mathcal{D}(\mu_\theta(\mathbf{x}_t, t, c), c^s) = \frac{\sum_i \sum_j O_{ij} \mathcal{K}(c_{ij}^s - \mu_{ij}^g)}{\sum_i \sum_j O_{ij}} \quad (5)$$

Here,  $O_{ij}$  is a boolean value representing if at frame  $i$ , joint  $j$  is controlled. The predicted mean is transformed into a global joint representation  $\mu^g$  and assessed with the control signal  $c^s$  in the same format under a pre-defined loss calculation function  $\mathcal{K}$ , suitable for different circumstances, ensuring that joint positions align with the spatial control requirements from a global perspective in both time and layout. Additionally, since gradient updates target the mean  $\mathbf{x}_t$  in a relative motion representation, these updates are naturally propagated across all time frames and joints throughout the motion sequence. This coherent propagation facilitates a natural adjustment of the entire body’s joints, even when only a few joints are being actively controlled and edited.